

# GaAs Based Type II Heterostructures\*

R. Planel

*Laboratoire de Microstructures et Microélectronique, Centre National de la Recherche Scientifique (L2M-CNRS)*

*BP107, 92225 Bagneux, France*

Received July 12, 1993

Heterostructures based on the GaAs/AlAs alloy system exhibit a staggered band alignment, as far as conduction states with X symmetry are concerned. This paper reviews the main features of the electronic states in such cases and presents, as an example of engineered non-linearity, an optically bistable "Type II quantum well" structure.

## I. Introduction

The GaAs/AlAs system was evidenced to be potentially of type II in 1986<sup>[1,2]</sup>. It has the unique advantage to be continuously compatible with the canonical type I system based on the same family of host materials. Due to the small lattice mismatch between GaAs and AlAs, Ga<sub>1-x</sub>Al<sub>x</sub>As alloys with any Aluminium concentration  $x$  may be epitaxially grown on the same layers, with excellent control of thicknesses and concentrations. Thus, the epitaxial grower may create a wide variety of structures, in the spirit of engineering peculiar properties. He may use the spatial separation of carriers in different layers of the structure to create electric fields, which enhance the non-linear optical properties of the structure.

In Section II, we recall the basic features of the band structure and electronic states of these structures, on the basis of experimental results obtained in GaAs/AlAs short period superlattices (SL). In Section III, we present an experimental study of a more sophisticated structure where charge transfer has been used to obtain a specific non-linearity, optical bistability.

## II. Band structure and electronic states

Superlattices (SL) made of GaAs and AlAs were first investigated by several groups<sup>[1,2,3]</sup> for probably several reasons. First, these SL could be considered as a good alternative to thick Ga<sub>1-x</sub>Al<sub>x</sub>As alloys, especially in optical devices such as lasers and waveguide modulators; this is because the technology of growth

reveals easier to control, especially to reach high Al content alloys. Second, the growth of thick superlattices allows rapid post-growth characterization using X-ray diffraction. This is of central interest to compare experimental results with the theory. Actually, these studies provided an excellent experimental checking of the Envelope Function Approximation (EFA) developed by Bastard<sup>[4]</sup>. This theory is an essential tool for prevision and engineering.

A special motivation<sup>[2]</sup> was to get a precise value ( $\Delta E_C/\Delta E_G = 0.67$ ) of the offset ratio parameter in the GaAs/AlAs system, which was still in that period a matter of controversy. As a matter of fact, the ability to get type II structures was closely linked to the band offset between the two host materials, since it would not have been possible with the so-called Dingle's value of this offset (0.85) proposed in the earlier studies of type I GaAs/GaAlAs Quantum Wells (QW). The key feature is the following: the X conduction band extremum of AlAs bulk material lies at lower energy than the equivalent extremum in GaAs. This feature can be easily complemented with the reasonable approximation of a linear variation of the X-energy in Ga<sub>1-x</sub>Al<sub>x</sub>As alloys. On the other hand, except the confinement of the spin-orbit split-off states<sup>[5]</sup>, the situation of valence states is not substantially different in GaAs/AlAs heterostructures from the case of GaAs/Ga<sub>0.65</sub>Al<sub>0.35</sub>As: holes are confined in the GaAs layers. This allows to assert that heterostructures built in this system may be of type II, as far as X-potential profiles are concerned. This happens either when indirect materials are used (i.e. with  $x > 0.35$ , typically), or when confinement effects rise the  $\Gamma$  states at high enough energy for the X-states to

---

\*Invited talk.

become the conduction fundamental state.

Systematic experimental studies of GaAs/AlAs SL have been done, mainly by mean of cw photoluminescence (PL), and excitation spectrum of luminescence (PLE). Roughly speaking, the former provides the basic information on the gap between valence states and the lower conduction states, of X-symmetry in the case of type II SL. The latter, which is more or less equivalent to absorption spectroscopy, provides the direct-type I energy gap, where strong absorption begins. The conclusion of these systematic studies may be drawn as in Fig 1. The GaAs/AlAs superlattice is direct and type I if the GaAs layer thickness  $L_{\text{GaAs}}$  is larger than 3.5 to 4 nm or if the average Aluminum concentration  $x$  (defined as  $L_{\text{AlAs}}/(L_{\text{GaAs}}+L_{\text{AlAs}})$ ) is smaller than 0.35, the critical concentration for direct to indirect gap transition in  $\text{Ga}_{1-x}\text{Al}_x\text{As}$  alloys ( these numerical values are slightly dependent on temperature, since the X and  $\Gamma$  temperature coefficient are very different). The second criterion is of course more efficient for very short period SL's, which may be considered as "pseudo-alloys".

If the structure parameters lie outside this region, the structure is of type II, and the band gap energy provided by excitation spectroscopy appears significantly higher than the photoluminescence energy. This case was often said "indirect in li-space and in real space". As we shall see now, this assertion is not appropriate, for two reasons, which are intimately related.

For a more accurate understanding of the X-conduction state, it has been necessary to rely on time resolved luminescence<sup>[6]</sup> and uniaxial strain perturbation<sup>[7]</sup>. The features are somehow intricate because of the small lattice mismatch between the bulk materials GaAs and AlAs, which results in a biaxial strain of AlAs to match the lattice constant fixed by the GaAs substrate. This lowers the energy of the  $X_{x,y}$  extrema of the AlAs band structure (which are situated in k-directions 100 and 010, within the plane of the layers), with respect to the  $X_z$  one (which lies along 001, the growth direction). Such energy extrema are highly anisotropic, with cigar-like constant energy surfaces. As a consequence, the confinement effect rises the  $X_{x,y}$  energy in a more pronounced way than the  $X_z$  energy. It is the balance between confinement and strain effects which will determine the symmetry of the fundamental X-states. Thus, in an heterostructure, the  $X_z$  states

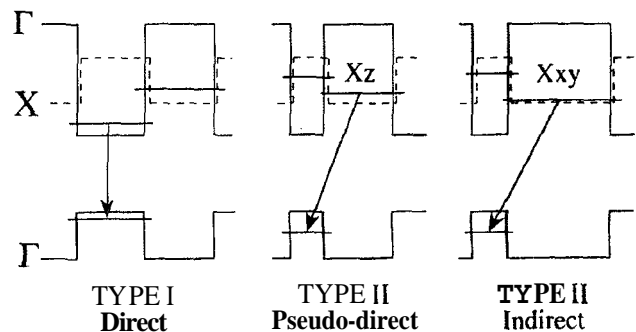
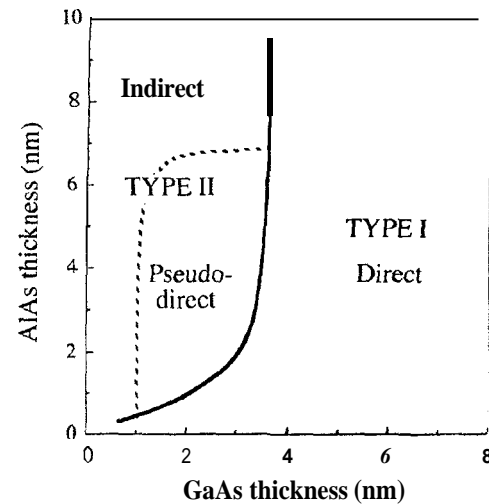


Figure 1, lower: Band extrema profiles of GaAs/AlAs Superlattices, sketching the three main types of structures. upper:  $L_{\text{AlAs}}$  versus  $L_{\text{GaAs}}$  map showing the three main regions of interest.

do not retain a periodic term in their envelope-function, due to the folding of the Brillouin zone; and some non-zero overlap may exist between conduction and valence envelope functions. Experimentally, it expresses very clearly into an intense zero-phonon recombination appearing on the PL spectra, and a more rapid decay (typically  $1\mu\text{s}$ ) than for  $X_{x,y}$  states ( $100\mu\text{s}$  to  $1\text{ms}$ )<sup>[6]</sup>. The  $X_z$  recombination can be said pseudo-direct, since direct recombination, without phonon emission, is allowed by the heterostructure potential, although the system remains of type II. Thus, it has been possible to determine both regions in the  $L_{\text{AlAs}}$  vs.  $L_{\text{GaAs}}$  map of Fig. 1. The SL fundamental conduction states are  $X_{x,y}$  like, if  $L_{\text{AlAs}} < 7\text{nm}$ , or for very thin  $L_{\text{GaAs}}$ , typically  $< 111111$ .

### III. Optical bistability

Since several years ago, new tools for "band gap engineering" are available in this well controlled family of

materials; for instance, an indirect-to-direct transition has been observed in a GaAs/AlAs superlattice under external electric field<sup>[8]</sup>, with consequences on the photoluminescence intensity. As a further example, in a more sophisticated and asymmetric structure, spatial separation of charges has been demonstrated to create an internal electric field with subsequent action on the photoluminescence emission energy of a type I QW<sup>[9]</sup>.

I describe now a structure which exhibits all-optical bistability in photoluminescence, with huge variation of intensity and spectrum. These results have been presented in more details in<sup>[10]</sup>. The bistability is observable without any external field, but electrical measurements and switchings are also possible. Zrenner and coworkers<sup>[11]</sup> have observed a similar effect under external electric field, thought to be due to hot carriers. On the basis of luminescence spectrum analysis, and of electrical measurements, we propose a different explanation: each state corresponds to a different quasi static charge distribution within the heart of the structure; and switching as well as bistability are explained in terms of charge accumulation and associated electric fields.

The structure, which was grown by Molecular Beam Epitaxy, consists of a n-i-n sequence, in which the intrinsic region is made of four layers, as described and labelled in Fig. 2a. It may be viewed as one "Type-II indirect quantum well" imbedded into a  $\text{Ga}_{0.65}\text{Al}_{0.35}\text{As}$  alloy, which acts as effective left (LB) and right (RB) barriers for  $X$ -as well as  $\Gamma$ -electrons. The relevant energies, modified by the carrier confinement, are also given in Fig 2a. These quantities have been obtained using a transfer-matrix calculation<sup>[12]</sup>, based on the Envelope Function Approximation.

These are values obtained without carrier population, and they should be modified under photoexcitation. Two terms are competing to modify the energy gaps: The band gap renormalization on one hand, which tends to close it, and the electrostatic term (Hartree term), which tends to open it. Recent experimental and theoretical studies<sup>[13]</sup> show that the former may be neglected in Type II structures with wide enough AlAs layers (typically  $L_{\text{AlAs}} > 5\text{nm}$ ). Our transfer-matrix calculation may account for electric fields which are present in the structure. Thus, through the self-consistent coupling with Poisson equa-

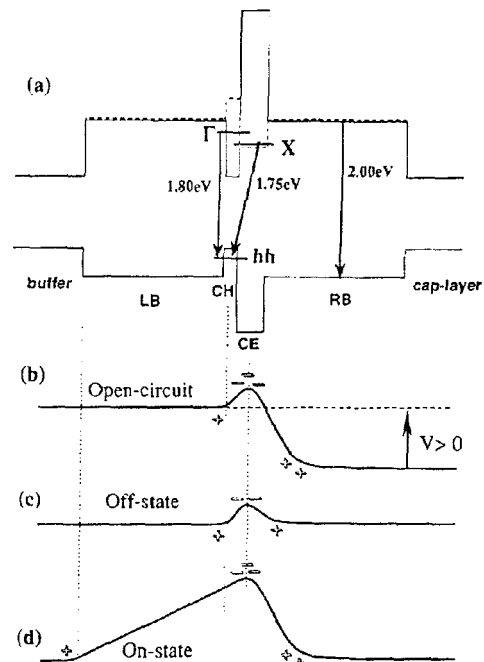


Figure 2: a) The structure is made of the following layers: Buffer and cap layers (n+-GaAs); LB and RB: ( $\text{Ga}_{0.65}\text{Al}_{0.35}\text{As}$ , 100nm); CH (GaAs, 2.5nm); CE (AlAs, 10nm). The potential profiles for  $\Gamma$ -electrons and holes (solid line) and  $X$ -electrons (dashed line) are shown, with the main transition energies. Below: Electric potential profiles: b) in an open-circuited diode. Estimated charge densities are, from left to right: CH:  $7.10^{11}\text{cm}^{-2}$ ; CE:  $3.7 \cdot 10^{12}\text{cm}^{-2}$ ; and RB:  $3.10^{12}\text{cm}^{-2}$  c) in a short-circuited diode in the OFF-state. Estimated charge densities are: CH:  $7.10^{11}\text{cm}^{-2}$ ; CE:  $1.1 \cdot 10^{12}\text{cm}^{-2}$ ; and RB:  $4.10^{11}\text{cm}^{-2}$  d) in a short-circuited diode in the ON-state. Estimated charge densities are: buffer:  $2.10^{11}\text{cm}^{-2}$ ; CE:  $3.2 \cdot 10^{12}\text{cm}^{-2}$ ; and RB:  $3.10^{12}\text{cm}^{-2}$ .

tion, we get a reasonable quantitative description of the carrier population effects on the electronic levels of the structure. The principle of the calculation is sketched in Fig. 3. Although it cannot be presented and discussed in details here, this calculation was a great help for discussion of the experimental results. It indicates that we may obtain a 6 meV blue-shift of the  $X$ -HH energy, due to the photocreated electrostatic potential, for both electron and hole densities equal to  $10^{11}\text{cm}^{-2}$ . Another consequence of the optical excitation is the filling of the two-dimensional state densities ( $3.8 \cdot 10^{11}\text{cm}^{-2}/\text{meV}$  for  $X_{x,y}$  electrons and  $0.39 \cdot 10^{11}\text{cm}^{-2}/\text{meV}$  for holes), which leads to the consideration of the two associated pseudo Fermi levels (PFL).

We have studied the PL and PLE of this sample at low temperature (5K). Electrical measurements under

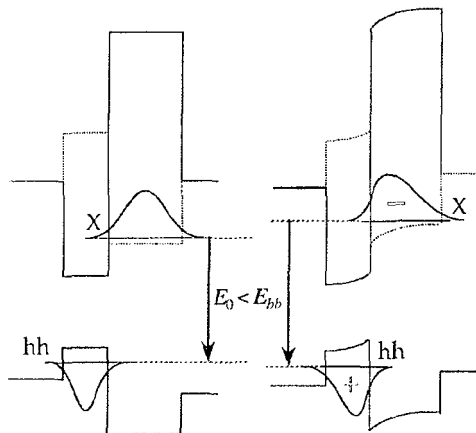


Figure 3: Band extrema profiles and envelope functions of photo-created carriers in a type II quantum well, without (left) and with (right) account of the band bending due to the electrostatic (Hartree) interaction.

optical excitation have also been made, with simultaneous recording of the PL. For that purpose, mesa-type diodes were fabricated by conventional lithography and etching.

The PL consists of two main lines (see fig 4): one (at about 1.80 eV) is attributed to recombination in the type II QW, the other (at about 2.00 eV) to recombination in the barrier layers. Two different stable states are found in the 40 to 250 W/cm<sup>2</sup> range of exciting power  $P_{ex}$ . The most prominent distinction is found on the barrier recombination. It is of interest to detail the evolution of the type II QW recombination (see Fig.5): For very weak excitation ( $P_{ex} \sim 1$ W/cm<sup>2</sup>), one observes the spectrum characteristic for a type II indirect recombination, involving electrons with  $X_{x,y}$  symmetry: a weak zero-phonon recombination (1740 meV), associated to three more intense phonon replica at lower energies. We can also observe the  $\Gamma$ -HH direct-type I transition in the GaAs CH QW (1820 meV). For  $P_{ex} > 5$ W/cm<sup>2</sup>, we observe the luminescence associated to the population of the  $X_z$  electronic level. The type II transitions experience a characteristic strong blue shift, while the type I line is slightly red shifted by the band gap renormalization. Thus, as  $P_{ex}$  reaches, typically, 100 W/cm<sup>2</sup>, the type II luminescence merges into the  $\Gamma$ -HH line and the total intensity of radiative recombination from the central cell of the structure increases rapidly. The theoretical description presented above allows us to associate these shifts with charge densities present in the layers. Under both actions of photocre-

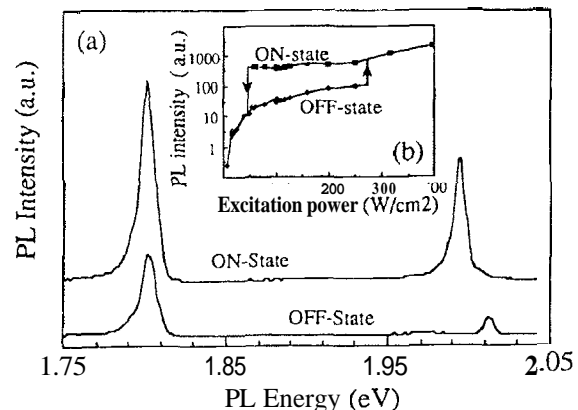


Figure 4: a) PL OFF- and ON-spectra of the bistable structure for  $P_{ex} = 100$ W/cm<sup>2</sup>. b) Hysteresis loop versus  $P_{ex}$  of integrated PL in the 1950 to 2050 meV range.

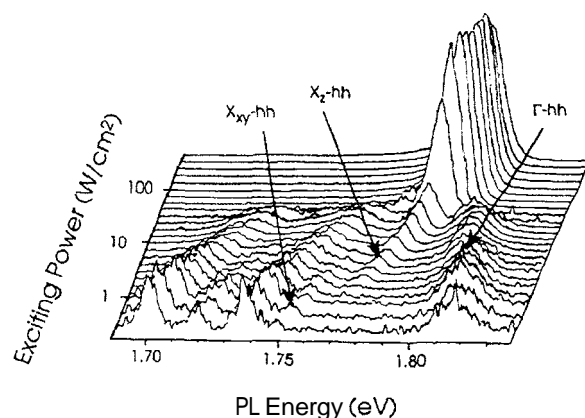


Figure 5: PL spectra of the type II QW as a function of the exciting power. The integrated PL intensity of each spectrum has been normalized. Bistability occurs when the  $X$ -HH and  $\Gamma$ -HH lines merge.

ated electrostatic potential and level filling, the  $X$ -PFL in CE-layer is lifted up to the  $\Gamma$ -level in CH-layer. The saturation appears, for  $P_{ex} \sim 100$  W/cm<sup>2</sup>, when the  $\Gamma$  level is populated, allowing fast  $\Gamma$ -HH recombination. We estimate the required densities at  $7 \cdot 10^{11}$ cm<sup>-2</sup>.

On view of these results, we are led to the following proposal, which is sketched in Fig. 2: The OFF and ON states correspond respectively to weak or strong accumulation in the RB-layer, most probably in the triangular attractive potential created by the accumulation of electrons in the CE-layer (this triangular well may be compared to those appearing in modulation-doped heterojunctions, and explains the low energy broadening of the barrier luminescence in the ON state).

To explain first the open-circuit behavior we have to point out that electrons can be collected in the CE-

layer from both sides of the structure, whereas holes photo-created in the RB-layer cannot be collected into the CH-layer because of the AlAs barrier in the valence band. It gives rise to an excess hole population in the RB-layer, and then to a positive photovoltage. This explains the strong barrier PL. In the LB-layer, both electrons and holes can move freely, then any electric field in this layer would be screened as far as charge accumulation is possible in the adjacent layers. Fig. 2b shows the resulting potential profile.

We now discuss a possible mechanism for switching between the two states and for bistability, which rely on the distribution of charges and electric fields in the heart of the structure when the diode is short-circuited. At low  $P_{ex}$ , RB-holes in excess must flow towards the cap layer (on the right), to ensure the alignment of the Fermi level of both n-doped region of the n-i-n structure. It generates a positive photo-current, and leads to reduction of the RB PL intensity, with respect to the open circuit situation. In other words, as charges accumulate, the two potential drops adjacent to the type II QW are kept opposite (see Fig. 2c). This corresponds to the OFF state.

When  $P_{ex}$  increases, the  $\Gamma$ -HH recombination comes into play, as shown in Fig.5, which drastically reduces the lifetime of CH-holes. That leads to the emergence of an electric field in the LB-layer to hold equal potentials in the two electrodes. Thus, the RB-hole population may increase. Because of the large thickness of the LB-layer (100 nm), a much larger potential difference may be created between the buffer electrode and the CE-layer with the same charge quantity. As a consequence, the limit to the accumulation of holes at the CE-RB interface disappears: this characterizes the ON-state (Fig.2d). This abrupt change in the charge distribution and potential profile of the structure is detected by two PL features: i) a steep increase of the Type II QW emission, which indicates that holes from the LB-barrier are collected in the CH layer with a better efficiency, typically twice higher (but this does not imply an increase of the CH-layer population, due to the correlative decrease of their radiative lifetime); ii) a large increase of the  $Ga_{0.65}Al_{0.35}As$  barrier PL, due to the high accumulation of holes at the CE-RB interface.

It is essential, at this stage, to consider that the LB electric field does raise the electron X energy (in the

CE layer) with respect to the  $\Gamma$  one (in the CH layer). This provides the positive feed-back necessary to get bistability.

#### IV. Conclusions

Thus, we are allowed to play with charge distributions in Type II structures. The example of this bistable structure retains their main advantages. The threshold values are at least two orders of magnitude lower than in current devices based on more classical optical non-linearities, acting for example in the active layer of Fabry-Perot resonators<sup>[14]</sup>. This is due to the slow recombination rates of spatially separated carriers. Another important point is that the structure parameters and experimental conditions are not as critical. On the other hand, as far as potential applications to devices are concerned, this advantage is counterbalanced by slow recovery when excitation is switched off. This is a general limitation in device physics. And the optimization of these various criteria for a given practical application is still to be done.

#### Acknowledgments

Many studies reviewed in this paper have been done in L2M-CNRS by several coworkers, mainly G. Danan, M. Jezewski, F. Mollot, and R. Teissier. I also reported the fruits of many collaborations, especially with C. Beiloin à la Guillaume from GPS (Université Paris 7) and B. Gil from GES (Université de Montpellier II).

#### References

1. E. Finkman, M. D. Sturge, and M. C. Tamargo, *Appl. Phys. Lett.* 49, 1299, (1986).
2. G. Danan et al. *Proc. 18th Internat. Conf. Phys. Semicond.*, Stockholm 1986, edited by O. Engström, (World Scientific, Singapore, 1987) p. 719 ; *Phys. Rev. B* 35, 6207 (1987).
3. K. J. Moore, P. Dawson, and C. T. Foxon, *J. Phys. (Paris) C5*, 525 (1987); *Phys. Rev. B* 38, 3368 (1988).
4. G. Bastard, *Phys. Rev. B*, 24, 5693, (1981); *Wave Mechanics Applied to Semiconductor Heterostructures*, (Les Editions de Physique, Les Ulis 91-France, 1988).

5. J. Barrau, K. Khirouni, Th. Amand, J.C. Brabant, B. Brousseau, M. Brousseau, Phi Hoa Binh, F. Mollot and R. Planel. *J. Appl. Phys.* **65**, 3501 (1989).
6. D. Scalbert *et al.*, *Solid State Com.*, **70**, 945, (1989); M. Maaref *et al.* *Phys. Stat. Sol.*, **170**, 637 (1992).
7. P. Lefebvre, B. Gil, H. Mathieu and R. Planel, *Phys Rev.* **B39**, 5550 (1989); *Phys. Rev.B* **40**, 7802 (1990).
8. M. H. Meynadier *et al.* *Phys. Rev. Lett.* **60**, 1338 (1988).
9. M. Jezewski, R. Teissier, F. Mollot, R. Planel, *Superlatt. and Microstruct.* **8**, 320 (1990).
10. R. Teissier, R. Planel, and F. Mollot, *Appl.Phys.Lett.* **60**, 2663 (1992).
11. A. Zrenner, J. M. Worlock, L. T. Florez, and J. P. Harbison, *Appl. Phys. Lett.* **56**, 1763 (1990).
12. Yuh Peng-Fei and K. L. Wang, *Phys. Rev.* **B38**, 13307 (1988).
13. K. Boujdaria, Thèse de l'Université Paris 7, to be published.
14. See for example B. G. Sfez, J. L. Oudar, J. C. Michel, R. Kuszelewicz, and R. Azoulay, *Appl. Phys. Lett.* **57**, 4, 324 (1990).